Modeling and Simulation of Thermal Effects on Electrical Behavior in Lithium-Ion Cells

Cristóbal E. Allendes[1], Ammi Beltrán[2], Jorge E. García Bustos[3], Diego Troncoso-Kurtovic[4], Bruno Masserano[5], Benjamín Brito Schiele[6], Violeta Rivera[7], Francisco Jaramillo[8], Marcos E. Orchard[9], Jorge F. Silva[10], Heraldo Rozas[11] and Srikanth Rangarajan[12]

[1,2,3,5,6,7,11] *Department of Electrical Engineering, Universidad de Chile, 8370456 Santiago, Chile*
cristobal.allendes@ug.uchile.cl
ammi.beltran@ug.uchile.cl
jorgegarcia@ug.uchile.cl
bruno.masserano@ug.uchile.cl
benjamin.brito@ug.uchile.cl
violeta.rivera@ug.uchile.cl
heraldo.rozas@ug.uchile.cl

[1,3,4,5,6,8,9,10] *Center for Sustainable Acceleration of Electromobility - CASE, Universidad de Chile, 8370456 Santiago, Chile*
diego.troncoso.k@ug.uchile.cl
francisco.jaramillo@ing.uchile.cl
morchard@u.uchile.cl
josilva@ing.uchile.cl

[12] *Binghamton University, Binghamton, New York, 13901, United States of America*
srangar@binghamton.edu

ABSTRACT

Thermal effects exert a crucial influence on the electrical behavior of lithium-ion batteries, significantly impacting key parameters such as the open circuit voltage curve, internal impedance, and cell degradation rate. Furthermore, these effects may give rise to electrolyte loss, resulting in a reduction in capacity. The cycling of batteries inherently generates internal heat, establishing a direct relationship between cell temperature and power demand. This article aims to provide a methodology to model electrothermal relations and temperature influence on electrical behavior in lithium-ion cells, as well as a simulation of extended cell operation under arbitrary power loads, presenting a novel approach not previously explored. It does this by considering three models: the Bernardi model for heat generation within the cell, a thermal lumped model for the cell's temperature, and the Vogel-Fulcher-Tammann model for the capacity change as a function of temperature. These models are then connected to a state-of-the-art open circuit voltage model of a cell, providing a connection from the thermal world back into the electrical world. Experiments with different power demands occur on the simulation, including estimation of thermal parameters with relative errors under $1\,\%$, visualizing the effects of the integrated models and potential for real-cell applications.

1. INTRODUCTION

When designing lithium-ion battery systems, temperature and heat generation are critical factors that influence the electric behavior. These changes in how a cell behaves subsequently affect the degradation and efficiency of battery energy storage systems (Spitthoff, Shearing, & Burheim, 2021). Also, extreme temperatures significantly increase the degradation processes (Hou, Yang, Wang, & Zhang, 2020), with the cell's internal heat generation and the environment's impact on heat release influencing these processes. The connection of these effects thus creates a complex interdependence between thermal and electrical phenomena.

The degradation of lithium-ion batteries significantly impacts their thermal and electrical characteristics. Various methodologies have been proposed to assess this degradation, which depend on factors such as the amount of available data, ac-

cessibility to the cell, equipment, and expert knowledge. The State of Health (SoH) is commonly employed as an indicator, defined as the ratio between the current capacity of the cell and its initial or nominal capacity.

$$\text{SoH} = \frac{Q_i}{Q_0}, \tag{1}$$

where Q_i and Q_0 represent the current and initial capacities, respectively.

Accurately estimating the SoH is crucial for operational purposes, as determining the current capacity is essential for estimating the remaining charge within a cycle. To achieve this, the State of Charge (SoC) is widely utilized in the literature and can be represented as follows:

$$\text{SoC}(t) = \text{SoC}(0) - \frac{1}{Q_0}\int_0^t I(t)\,dt \tag{2}$$

where:

- $\text{SoC}(t)$ is the state of charge at time t.
- $\text{SoC}(0)$ is the initial state of charge.
- Q_0 is the nominal capacity of the battery.
- $I(t)$ is the current flowing out of the cell at time t.

The chemical reactions that cause the cell's degradation are evidenced by a reduction in battery capacity, change in the Open-Circuit Voltage (OCV) curve and an increase in internal resistance. Therefore, monitoring these variables offers a direct method for estimating the SoH.

In the Prognostics and Health Management (PHM) area, several studies have laid the foundation for thermal and electrochemical modeling work, which seeks to improve the prognostic capabilities of essential variables of lithium-ion batteries. In Wang et al. (2023), the authors explore using different data-driven architectures to predict the temperatures inside a lithium-ion battery accurately. However, it is important to note that these predictions, while accurate, are only valid within a limited operational range. Even though the implemented neural networks achieve an accurate predictive performance, those predictions do not consider how temperature affects the dynamics of the cell's SoC or effective capacity. Similarly, Damay, Forgez, Bichat, Friedrich, and Ospina (2013) provides valuable insights with their lumped parameter thermal model that simulates the behavior of individual cells. Although their model aligns well with experimental validations, it may not accurately represent the impact of temperature on cell capacity, potentially leading to misestimations of the SoC under varied thermal conditions. Furthermore, Akbarzadeh et al. (2020) developed a model that characterizes the thermal behavior of a high-energy prismatic lithium-ion module by considering a lumped parameter model of the individual cells. Although the presented model behaves well under validation measurements, since the impact of temperature on the cell's capacity is not considered, the SoC dynamics might be misrepresented when operating under high-temperature conditions.

Additionally, Zhu et al. (2023) constructs a fractional-order electrochemical model of a lithium-ion battery, aiming for computational efficiency and precision. Even though they achieved good performance in terms of model accuracy and computational efficiency, the model formulation assumes a fixed battery capacity, potentially leading to biased estimations of the SoC for batteries, particularly in environments where temperature control is challenging. Moreover, Hoelle, Dengler, Zimmermann, and Hinrichsen (2023) models the thermal behavior of a lithium-ion battery with a three-dimensional distributed simulation. The main focus of the research is accurately characterizing temperature dynamics along the different components of the battery, especially during thermal runaways. Still, the simulation does not consider heat generation from electrical sources and its high computational cost renders it impractical for online applications. Similarly, Li, Wang, Duan, Li, and Wang (2022) reviews several studies that use the battery's electrochemical impedance spectrum for heat generation prediction under various conditions. Although this method is accurate and holds potential for online estimation schemes, the thermal effect on the battery capacity is neglected. Also, precise impedance measurements are often achieved with expensive laboratory equipment, hindering their implementation in industrial applications, like electromobility. Finally, Yang, Patil, and Fahimi (2019) explores the electrothermal effects in lithium-ion batteries for electric vehicles, empirically testing the importance of electric profiles in heat generation inside the battery. However, this research does not deeply inquire how thermal variables affect electrical variables such as capacity and internal impedance, thus yielding an incomplete model.

Despite the documented relationship between thermal and electrical phenomena, previous studies often work on these areas separately without fully encompassing their influences. This interrelationship is vital for an accurate prognosis of the operational variables of lithium-ion cells (Barcellona, Colnago, Montrasio, & Piegari, 2022).

This work aims to shorten the gap above by considering known and well-validated electrical and thermal models, adding to them to better model realistic usage scenarios, and integrating them into an electrothermal model that takes into consideration how the electrical and thermal world affect each other, thus seeking to improve the understanding of these interactions and also facilitate the prognostic of the SoC and SoH. This research effort proposes several significant advancements in the electrothermal modeling of lithium-ion batteries, aiming to enhance both the theoretical understand-

ing and practical applications of battery health management. The key contributions of this study are itemized as follows:

Improved Heat Model: While the simplest thermal models, such as the ohmic heat model represented by $q = R_T I^2$ where q is the generated heat, R_T is the internal resistance and I is the current through the cell, primarily account for resistive heating, they often overlook the entropic heat contribution, which can become significant over extended periods and numerous cycles. In particular, high-current operations typically render this component negligible. This is supported by findings in Akbarzadeh et al. (2020), where the entropic term is excluded due to its minor contribution under their experimental conditions. However, our application's focus on forecasting necessitates the consideration of these subtle effects, which can lead to substantial deviations over time. This distinction is critical, particularly in predictive scenarios where the cumulative impact of entropic heating becomes increasingly significant. Therefore, our model innovatively incorporates an empirical approach to quantify these effects, substantially enhancing the precision of thermal management and thereby extending battery life in practical applications.

Temperature-Induced State of Charge Shifts: We analyze the impact of temperature variations on the SoC, providing insights into how thermal conditions affect battery capacity and discharge cycles.

Parameter Analysis for Model Implementation: In this study, parameter analysis for model implementation is essential to gain a comprehensive understanding of battery behavior under various conditions. The Vogel-Fulcher-Tammann (VFT) parameters, as derived from Lam, Bauer, and Kelder (2011), are pivotal in elucidating the temperature dependence of battery performance. Additionally, the open-circuit voltage (OCV) parameters, based on the work of D. Pola et al. (2016), facilitate accurate modeling of the electrical behavior under varying thermal conditions. Furthermore, the Entropic Heat Coefficient (EHC) has been shown to be independent of the cell type or temperature, making it applicable across different battery chemistries. The specifics of the thermal model are tailored to individual battery configurations, underscoring the necessity for customized thermal management strategies.

The article's structure consists of four main sections. Section 2 analyzes the theoretical framework, reviews existing models, and introduces the improvements and new models proposed in this work, focusing on the impact of the thermal and electrochemical behavior of lithium-ion batteries on their efficiency and capacity. Section 3 describes the methodology used for thermal parameter estimation, a simulation which includes the electrothermal models, as well as results from this simulator, demonstrating the capabilities and practical applications of the aforementioned models. Finally, Section 4 summarizes our research contributions, discusses the implications of our findings, and suggests future research directions.

2. ELECTROTHERMAL PHENOMENA AND PROPOSED MODELS

In this section, the existent electrical and thermal phenomena that appear within lithium-ion cells are presented, including how electrical usage profiles generate heat, how electrical parameters such as SoC affect battery performance, and how temperatures dynamically change within the cell, along with the contributions this work proposes to model such behaviors in a way that integrates both the electrical and thermal effects.

2.1. Entropic Heat Coefficient

Under a given electrical profile, the heat generated by a cell is modelled through the Bernardi model, where we consider the circuit model shown in Fig. 1 for the electrical behavior of a cell. While the model was originally proposed in Bernardi, Pawlikowski, and Newman (1985), the form given in Qian, Xuan, Zhao, and Shi (2019) and Paccha-Herrera, Calderón-Muñoz, Orchard, Jaramillo, and Medjaher (2020) is used, where the generated heat is given by

$$q_{\text{gen}} = I(V_{\text{oc}} - V) - IT\frac{\partial V_{\text{oc}}}{\partial T} = I^2 R_T - IT\frac{\partial V_{\text{oc}}}{\partial T}. \quad (3)$$

The leftmost term corresponds to irreversible heating caused by the Joule effect, while the rightmost term corresponds to reversible heating, caused by entropy variations within the cell (Paccha-Herrera et al., 2020). In this equation, I is the current flowing through the cell, where the convention that $I > 0$ indicates discharging and $I < 0$ indicates charging is used; R_T corresponds to the equivalent internal resistance of the cell, which can be measured through the use of an *Electrochemical Impedance Spectroscopy* (EIS) experiment for a particular cell; T is the internal temperature of the cell; V_{oc} is the open circuit voltage of the cell, and V is the terminal voltage of the cell.

Typically, the effects of the reversible heat are ignored under the assumption that $T\frac{\partial V_{\text{oc}}}{\partial T} \ll IR_T$ (He, Li, & Ma, 2014)

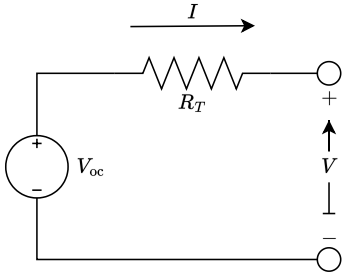

Figure 1. Circuit model used for the lithium-ion cell, based on a Thévenin equivalent circuit.

(Qian et al., 2019) (Akbarzadeh et al., 2020), which is a realistic assumption, especially for high currents. However, since the interest of this work lies on the applications of electrothermal models for prognosis, this effect should be considered: while the contributions of reversible heat are low on a per-cycle basis, these effects compound when long-term usage is considered, thus having a non-negligibe effect on end-of-life (EOL) prognosis.

The term $\frac{\partial V_{\text{oc}}}{\partial T}$ is called the *Entropic Heat Coefficient* (EHC), and it plays a crucial role in calculating reversible heating. In Paccha-Herrera et al. (2020) and Zhang, Song, and Feng (2013), EHC is measured by a potentiometric method, where the cell is left in an environment with a controlled ambient temperature, left to rest until thermal equilibrium is reached, and discharged by 10%, repeating this cycle for different temperatures until the cell is fully discharged. In those same works, it is shown that, for a given chemistry, temperature has a negligible effect on EHC, only showing a dependency on SoC. In Spitthoff et al. (2023), the relation between battery degradation and EHC is studied, and the results show that, while degradation does seem to have an effect on EHC, no clear pattern arises and the effects are negligible. These two observations point to the EHC as an intrinsic property of a given chemistry, which does not depend on temperature or degradation, motivating an empirical model where EHC only depends on SoC: in this work, the proposed novel EHC model is given by

$$\frac{\partial V_{\text{oc}}}{\partial T} \approx A \left[\frac{1}{\sqrt{2\pi\sigma^2}} \exp\left(-\frac{(\text{SoC} - \mu)^2}{2\sigma^2} \right) - \right. \\ \left. - \lambda \exp(-\kappa\, \text{SoC}) \right] + B \quad , \tag{4}$$

where $A, B, \sigma, \mu, \lambda$ and κ are shape parameters that have to be fitted to measurements of the EHC curve. Works such as Zhang et al. (2013) have proposed other empirical models for EHC, which were used as inspiration but the proposed model, during implementation, showed to be a better fit to the available data.

2.2. Lumped parameter thermal model

Purely thermal phenomena are modelled by a simplified lumped circuit analogue, proposed by Forgez, Vinh Do, Friedrich, Morcrette, and Delacourt (2010, Fig. 6b). The model is shown in Fig. 2, and it is taken directly from Forgez et al. (2010, Fig. 6b). It aims to model the internal and surface temperatures using three parameters, which have to be fitted to data from a given cell: heat capacity of the cell C_p, thermal resistivity between the internals of the cell and the surface R_{in}, and thermal resistivity between the surface and the environment R_{out}.

Since a circuit analogue is used in a context where electrical phenomena are also modelled, a different name is given for electrical and thermal resistances: electrical resistances are simply referred to as resistances, while thermal resistances are called resistivities, so as to avoid confusion between the two.

By analyzing the circuit analgoue, it can be seen that the model can be represented as the following Linear Time-Invariant (LTI) system

$$\dot{x} = -\frac{1}{C_p(R_{\text{in}} + R_{\text{out}})} x + \begin{pmatrix} \frac{1}{C_p(R_{\text{in}}+R_{\text{out}})} & \frac{1}{C_p} \end{pmatrix} \mathbf{u} \tag{5}$$

$$y = \frac{R_{\text{out}}}{R_{\text{in}} + R_{\text{out}}} x + \begin{pmatrix} \frac{R_{\text{in}}}{R_{\text{in}}+R_{\text{out}}} & 0 \end{pmatrix} \mathbf{u}, \tag{6}$$

where $x \equiv T_{\text{in}}$ is the hidden state (internal temperature), $y \equiv T_{\text{s}}$ are measurements taken at the surface of the cell, and $\mathbf{u} \equiv \begin{pmatrix} T_{\text{amb}} & q_{\text{gen}} \end{pmatrix}^\top$ are the inputs to the model.

An important aspect to take into consideration is that, while the lumped model takes the generated heat as an input, according to the rest of the models the heat would depend on the current temperature of the cell: thus, in reality, the system would be non-linear as the input would depend on the state. However, this can be circumvented in practice by using a heat profile that implicitly considers the rest of the effects, thus allowing the LTI model to be valid while keeping accuracy.

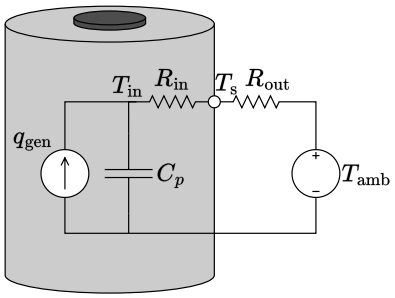

Figure 2. Simplified electrical analogue used for the lumped thermal model.

2.3. Capacity change with temperature

An electrolyte's electrical conductivity has been shown to depend on its temperature, with lower temperatures severely diminishing is conductivity and higher temperatures allowing for better electrical conductivity, which is crucial for battery performance given that a battery's electrical parameters are a function of electrolyte's conductivity, as well as other parameters. In Diederichsen, Buss, and McCloskey (2017), the electrolyte conductivity and temperature are related through the use of the VFT (Vogel-Fulcher-Tammann) equation, proposed by García-Coln, del Castillo, and Goldstein (1989) from the works of Fulcher and Tammann that were developed on top of Vogel's findings. In Lam et al. (2011), a slightly

modified VFT equation is proposed that models the relation between the usable cell capacity Q_{use} and the nominal cell capacity Q_0 as

$$Q_{\text{use}}(t,T) = Q_0(t)\exp\left(\frac{k_1}{T-k_2} - \frac{k_1}{T_{\text{ref}}-k_1}\right), \quad (7)$$

where k_1 and k_2 are empirically fitted parameters, and T_{ref} is the reference temperature at which the nominal capacity is measured. The nominal capacity $Q_0(t)$ corresponds to the cell capacity at the reference temperature, considering capacity loss due to degradation effects, while the usable capacity $Q_{\text{use}}(t,T)$ corresponds to the amount of charge that can be extracted from the cell at a given temperature T, considering the increases in electrolyte conductivity. It is extremely relevant to note that this increase in capacity is temporary, and does not consider electrolyte loss or lack thereof due to mechanisms such as electrolyte evaporation: thus, this limits the practical ranges at which the model can be considered valid, since it is known that extreme temperatures promote rapid degradation of the cell, as is shown in works such as Hou et al. (2020). Taking these permanent factors into consideration would require modelling the effects of temperature on $Q_0(t)$ on a cycle-to-cycle basis, which escapes the scope of the paper.

This VFT model was used by D. Pola et al. (2016) to implement a temperature-informed SoH prognostic framework using particle filtering, where it showed promising results, thus validating the use of the model for EOL prognosis.

In this work, it is established that the distinction between usable and nominal capacity gives rise to the notions of usable and nominal SoC, where the usable SoC corresponds to the charge left within the cell as a proportion of the usable capacity of the cell. These states of charge were observed to behave in such a way that a fully charged cell has the same usable and nominal states of charge, and as it discharges they begin to diverge: thus, this effect was named "SoC shift", and it is modelled by

$$\text{SoC}_{\text{use}}(t,T) = 1 + \frac{\text{SoC}_0(t) - 1}{\kappa(T)}, \quad (8)$$

where $\kappa(T) \equiv \exp\left(\frac{k_1}{T-k_2} - \frac{k_1}{T_{\text{ref}}-k_2}\right)$ comes from the VFT equation. Note that this definition causes nominal and usable SoC to match only at a full charge, and, as SoC drops, the curves differ between each other. SoC shift was defined in this way to better match experimental and predicted OCV curves, where the effect of temperature on OCV is more noticeable at lower states of charge.

Figure 3 shows how nominal and usable SoC relate to each other at different temperatures. At reference temperature, both states equal each other by definition but, as temperature increases, the usable SoC is higher than the nominal one, while at lower temperatures it is lower. For lower temperatures, a low nominal SoC results in negative usable SoC, which does not make physical sense but, in practice, it implies the possibility that low temperatures can lead to overdischarge when it is not expected: for example, at a temperature of -40 °C, while one might nominally think that the SoC of the cell is 20 %, in reality the usable SoC would be near 0 %, implying that the cell is fully discharged and, if kept being discharged, it puts the cell in the overdischarge regime, which has been shown to lead to permanent capacity loss and shorter life expectancy (Maleki & Howard, 2006).

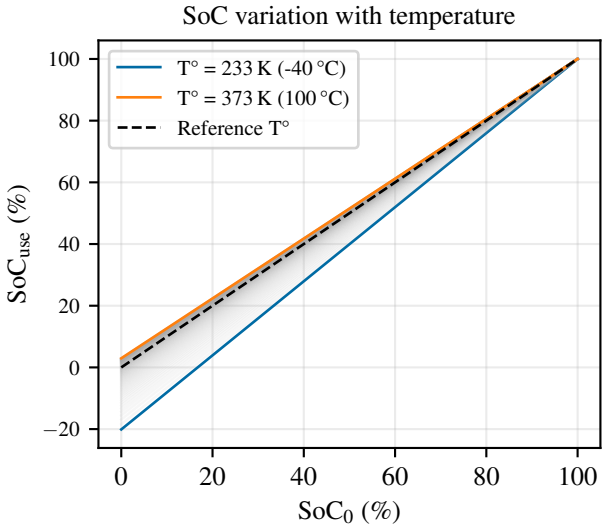

Figure 3. Difference between usable and nominal SoC predicted by SoC shift.

2.4. Open circuit voltage

The open circuit voltage is modelled as a function of SoC, by considering

$$V_{\text{oc}}(\text{SoC}) = v_L + (v_0 - v_L)e^{\gamma(\text{SoC}-1)} + \alpha v_L(\text{SoC}-1) + \\ + (1-\alpha)v_L\left(e^{-\beta} - e^{-\beta\sqrt{\text{SoC}}}\right), \quad (9)$$

where v_L, v_0, α, β and γ are estimated from battery data. This equation is proposed by D. A. Pola et al. (2015) with the goal of modelling the different areas of the OCV curve.

In order to incorporate thermal effects into the electric behavior, the usable SoC is used in Eq. 9 rather than the nominal one, thus introducing a dependency of OCV on temperature through SoC shifting. This model also has an effect on heat generation through the Bernardi model, presented in Eq. 3, by introducing a dependency of OCV on temperature: thus, a closed loop is formed, connecting the electrical and thermal worlds. The theoretical implications of this model can be seen

in Fig. 4, showing how OCV of the cell theoretically changes as a function of temperature, where it can be seen that, for any particular nominal SoC, OCV is directly proportional to cell temperature.

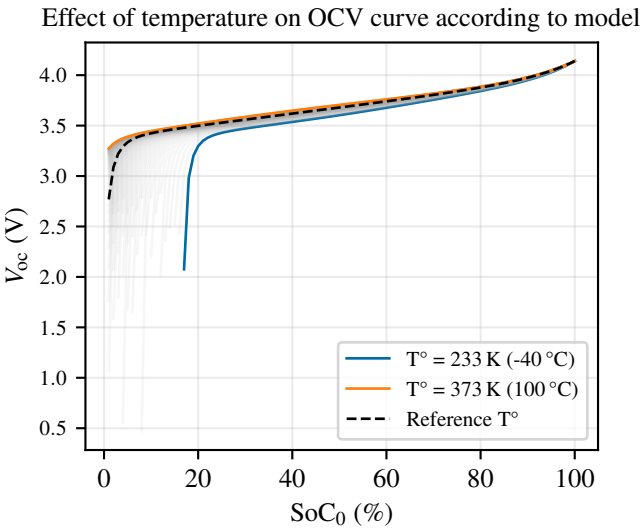

Figure 4. Predicted effect of SoC shift and EHC model on OCV curve.

3. MODEL VALIDATION

In this section, the methodology for the validation of the models using a simulated environment is described. This includes how thermal parameters are estimated from data, the design of the simulation itself, and the experiments that were performed within the simulation.

3.1. Parameter estimation for the different models

For the setup this work is interested in, most parameters are intrinsic to the cell to be experimented on, depending mostly on cell degradation and chemistry (two effects which are not being considered). These parameters include the ones for the heat generation and EHC model where, as was pointed out, EHC was shown to be an invariant of a given cell chemistry; and OCV, where it has been shown that the OCV characteristic of a cell mostly depends on degradation and temperature (the latter of which is being modelled in this work).

For VFT, not enough bibliography has been found to support the claim that, when applied to lithium-ion cells, the parameters of the model are only dependent on cell's chemistry. However, due to it modelling the cell's underlying electrolyte's conductivity, the reasonable assumption that they only depend on cell chemistry and degradation is made: thus, this work uses bibliographically available parameters for the simulation.

Lastly, there are the parameters for the thermal model. These are the most problematic because, unlike the previous ones, they are not only dependent on cell chemistry and degradation: they also depend on the configuration of the experiment itself, since a cell wrapped in a thermally insulating case would have a different thermal behavior than a cell in an open environment. Thus, these parameters have to be fitted for each experimental configuration. While Forgez et al. (2010) and Paccha-Herrera et al. (2020) used a method based on the permanent regime behavior of the models, in this work Least Squares (LS) regression is used to fit the three parameters of the thermal model.

The method for thermal parameter estimation is based on the LTI characterization of the model. Suppose the following LTI system is given

$$\mathbf{x}_{k+1} = \mathbf{A}_\theta \mathbf{x}_k + \mathbf{B}_\theta \mathbf{u}_k \tag{10}$$

$$\mathbf{y}_k = \mathbf{C}_\theta \mathbf{x}_k + \mathbf{D}_\theta \mathbf{u}_k, \tag{11}$$

where θ are the underlying parameters of the system (in this case, the thermal parameters). It can be seen that, while the system itself behaves linearly, it is not linear with respect to the underlying parameters, motivating the need for LS minimization. From dynamical systems theory, it is known that the response of the system can be expressed as

$$\mathbf{y}_{0:k} = \mathcal{A}_\theta(\mathbf{x}_0, \mathbf{u}_{0:k}), \tag{12}$$

where $\mathcal{A}_\theta(\cdot,\cdot)$ is the input-output operator, which is intrinsic to the system under parameters θ. Suppose the parameters θ^* of a given system are to be estimated from noisy measurements $\mathbf{y}_{0:k}$ under the known input $\mathbf{u}_{0:k}$ and initial conditions $\mathbf{x}_0$. Then, the estimated parameters $\hat{\theta}(\mathbf{y}_{0:k})$ are obtained by solving

$$\hat{\theta}(\mathbf{y}_{0:k}) = \arg\min_\theta \left\| \mathbf{y}_{0:k} - \mathcal{A}_\theta(\mathbf{x}_0, \mathbf{u}_{0:k}) \right\|^2. \tag{13}$$

This minimization is done in Python, by using the L-BFGS-B solver to minimize MSE under the constraint $\theta \succeq 0$ and using the *scipy* library to simulate $\mathcal{A}_\theta(\mathbf{x}_0, \mathbf{u}_{0:k})$ for some given parameters.

A relevant aspect to take into consideration is that proper estimation requires knowledge of the initial conditions $\mathbf{x}_0$, something which can not be taken for granted in most applications. However, for the particular problem this work is interested in, by letting the rest cell at a controlled ambient temperature until it reaches thermal equilibrium, the internal temperature converges to the surface temperature, thus allowing measurements of initial internal temperature to be taken.

3.2. Simulation of cell under load

A simulation of a lithium-ion cell was implemented in Simulink 2024a, following the diagram shown in Fig. 5. All the previously mentioned models, along with the contribu-

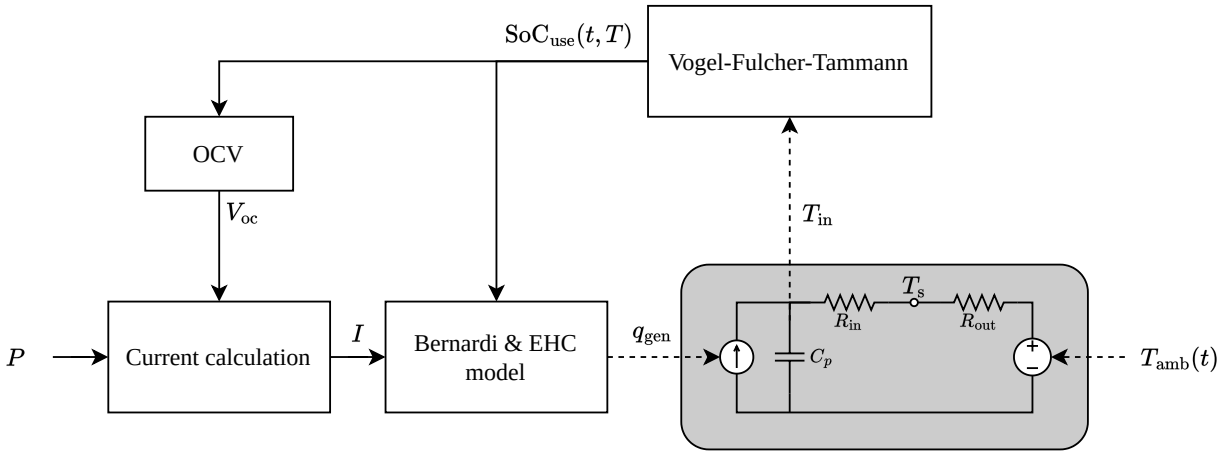

Figure 5. Diagram of the simulation, showing the models that were used, and how they were integrated with each other to produce real-time results.

tions from this work, were included in the simulation, thus introducing the interdependence between electrical and thermal phenomena that has been discussed.

The simulation consists of the model of a cell with two inputs: power and ambient temperature profiles over the desired simulation horizon. The parameters of the different models can be directly introduced into the cell, thus allowing the user to easily perform different experiments.

In Table 1, the parameters used for the different models in the simulation are shown along with their origin. Some of the parameters were obtained from bibliography, but thermal parameters were arbitrarily chosen within a reasonable range[1]. The effects of these thermal parameters has a large effect on the resulting shape of the outputs: however, the quality of the param

3.3. Experiments performed on the simulation

Two different experiments were performed on the simulation.

The first experiment has the purpose of testing the provided thermal parameter estimation. The cell starts at 0 °C and is then cycled under a constant ambient temperature of 25 °C. The cycling profile is shown in Fig. 6 which was chosen to accentuate the temperature differences between the cell, while giving it time to rest. Both the differences in the starting temperature and the input profile were chosen to maximize the information that the data carries of the parameters. The data is then contaminated with additive white Gaussian noise to better reflect a realistic scenario, and the parameters are estimated. The results of this estimation are shown in Table 2, and the measurements along with the fitted curve are shown in Fig. 8.

[1]To choose a reasonable range, the thermal parameters from Forgez et al. (2010) and Paccha-Herrera et al. (2020) were taken as a reference.

Associated model	Parameter	Value
Heat generation*	A	$4 \times 10^{-5}\,\mathrm{V\,K^{-1}}$
	B	$5 \times 10^{-5}\,\mathrm{V\,K^{-1}}$
	κ	3
	μ	0.4
	σ	0.05
	λ	7
	R_T	$0.12\,\Omega$
OCV**	α	0.15
	β	17
	γ	10.5
	v_0	4.14 V
	v_L	3.977 V
VFT***	k_1	-5.738 K
	k_2	209.9 K
	T_{ref}	298 K
Thermal****	C_p	$100\,\mathrm{J\,K^{-1}}$
	R_{in}	$3\,\mathrm{K\,W^{-1}}$
	R_{out}	$9\,\mathrm{K\,W^{-1}}$

(*) R_T was obtained from D. A. Pola et al. (2015, Table I), the rest were obtained by manually fitting the EHC curve shown by Paccha-Herrera et al. (2020, Figure 9)
(**) Obtained from D. A. Pola et al. (2015, Table I).
(***) Obtained from Lam et al. (2011, Table I).
(****) Arbitrarily chosen within a reasonable range.

Table 1. Parameters used for the different models in the simulation.

A relevant point to note is that the thermal model takes q_{gen} as an input, not the power profile. Thus, in order to perform the estimation, data from the generated heat must be extracted in order to properly include the electrothermal phenomena that was previously discussed.

The second experiment has the purpose of acting as a validation of the parameter estimation. A cell with the same

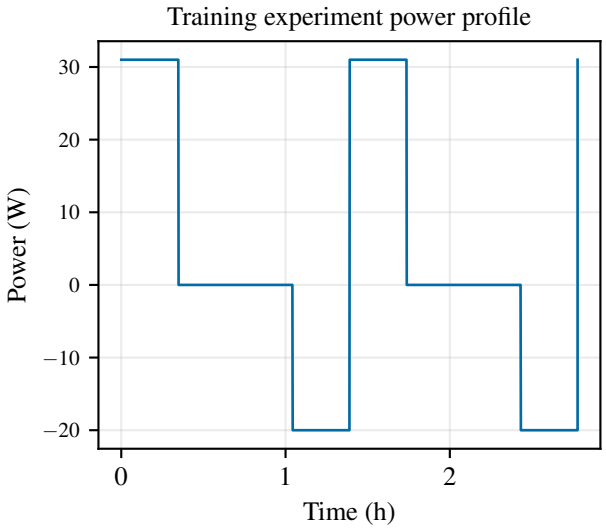

Figure 6. Inputs used for the experimental validation of the parameter estimation.

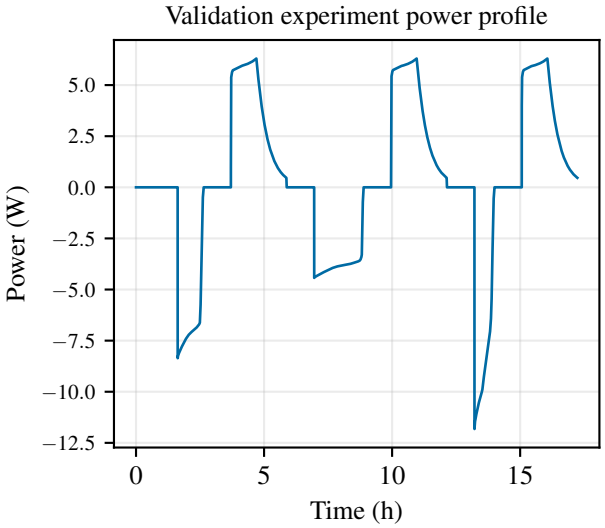

Figure 7. Inputs used as a validation of the generalizability of the estimation, taken from a realistic power profile.

parameters as the previous experiment is discharged under a semi-realistic power profile, in different testing conditions than those used for the parameter estimation. The previously estimated parameters are used, and the difference between the simulation with the real parameters and the one with the estimated parameters is shown. The power profile used as an input for this experiment is shown in Fig. 7, while the resulting temperatures, including the predicted internal temperature, are shown in Fig. 9.

Using both experiments, the measured and predicted temperatures are compared by considering RMSE and MAE as error metrics. The values for the metrics of each experiment are shown in Table 3.

From Table 2 and Figs. 8 and 9, the estimation of the thermal parameters proves to be satisfactory for this very reduced simulated scenario, with percentual errors in the estimated parameters under 1 % despite the artificial noise introduced into the simulation. In Table 3, both RMSE and MAE are under 1 °C for both the training and validation experiments, with the training metrics being higher due to the artificially introduced noise. However, further experimental validation in a non-simulated environment, with estimation of thermal parameters of a real cell, and comparisons of real and simulated curves, is required to show the wide applicability of the interconnected models to real world modelling and prognostics purposes.

4. CONCLUSIONS

In this work, four bibliographically available models of different electrical and thermal phenomena within lithium-ion cells were integrated, along with some extensions this work

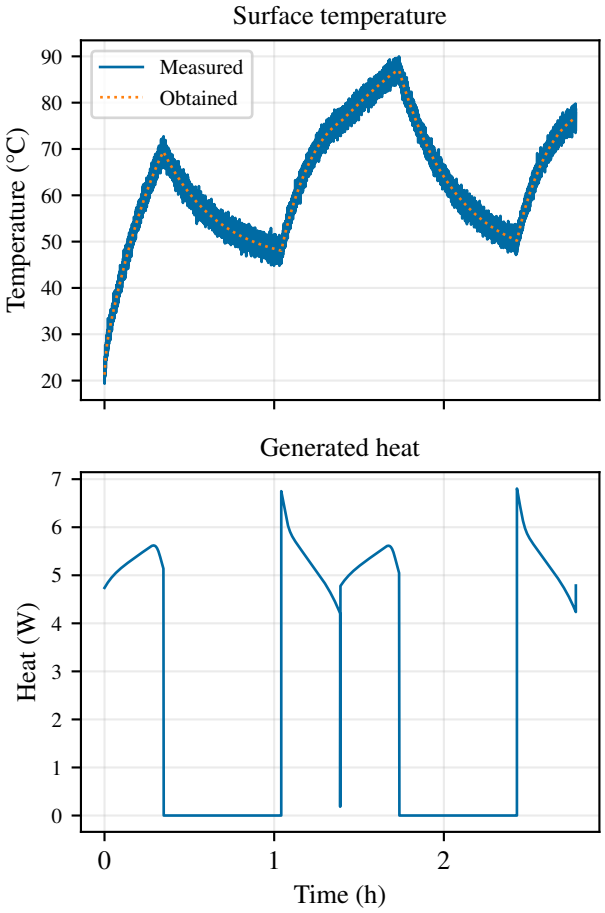

Figure 8. Outputs of the experimental validation of the parameter estimation, including the calculation of generated heat.

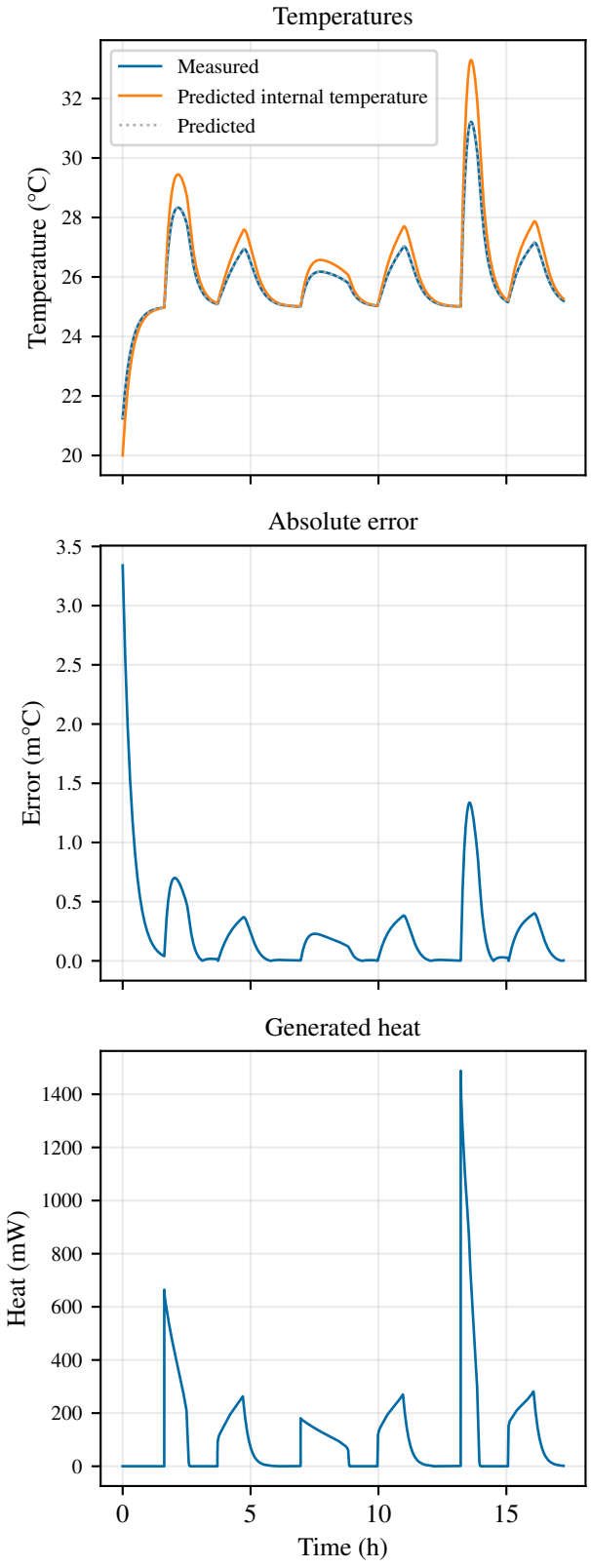

Figure 9. Outputs of the validation experiment, including the internal temperature predicted by the model and the absolute error at each timestamp.

Parameter	Expected	Estimated	Error (%)
C_p	$100\,\mathrm{J\,K^{-1}}$	$99.9040\,\mathrm{J\,K^{-1}}$	0.10
R_{in}	$3\,\mathrm{K\,W^{-1}}$	$3.0111\,\mathrm{K\,W^{-1}}$	0.37
R_{out}	$9\,\mathrm{K\,W^{-1}}$	$9.0009\,\mathrm{K\,W^{-1}}$	0.01

Table 2. Parameters estimated from simulated data, along with the percentual error.

	RMSE (°C)	MAE (°C)
Training	1	7.983×10^{-1}
Validation	4.6305×10^{-4}	2.487×10^{-4}

Table 3. RMSE and MAE from the training and validation temperatures. The training was performed with artificially introduced noise, explaining the difference in scales.

proposes. The following observed phenomena were linked together: how heat is generated within the cell due to electrical usage, using the Bernardi model and a proposed empirical entropic-heat coefficient model; how this heat generation, along with environmental factors, affect temperatures within the cell by considering a lumped parameter thermal model; how temperature causes changes in the usable capacity of the cell, introducing the phenomenon that this work named SoC shift, wherein temperature affects the perceived state of charge of the cell; and lastly, how SoC shift has an effect on the open circuit voltage characteristic of the cell, changing the electrical performance of the cell.

The integration of these different electrical and thermal phenomena, which had been previously worked on separately by other authors, results in a more complete electrothermal model of how a cell performs under temperature considerations, which could be used for more accurate diagnosis of relevant variables, such as temperature-aware state of health and prognosis of a battery's end of life.

A methodology for thermal parameter estimation from temperature measurements was proposed, and a simulation of a lithium-ion cell was developed, which included the previously named electrothermal phenomena. The estimation methodology was validated in a simulated environment with good performance and promising results, but the authors acknowledge the need for more validation under an experimental context, with real lithium-ion cells.

This motivates the need for future work, where the proposed models are validated with real lithium-ion cells in a controlled laboratory environment, which would allow the authors to explore the scalability of these models to larger and more complex battery configurations, more akin to industry-relevant scenarios such as electric vehicles' battery systems. Another key aspect to orient future work upon is studying the long-term effects of different thermal management solutions on battery degradation and reliability.

ACKNOWLEDGMENT

This work was supported in part by ANID FONDECYT 1210031, Advanced Center for Electrical and Electronic Engineering, ANID Basal Project FB0008. The work of Jorge E. García Bustos has been supported by ANID-PFCHA/Doctorado Nacional/2022-21221213.

REFERENCES

Akbarzadeh, M., Kalogiannis, T., Jaguemont, J., He, J., Jin, L., Berecibar, M., & Van Mierlo, J. (2020). Thermal modeling of a high-energy prismatic lithium-ion battery cell and module based on a new thermal characterization methodology. *Journal of Energy Storage*, *32*, 101707. doi: https://doi.org/10.1016/j.est.2020.101707

Barcellona, S., Colnago, S., Montrasio, P., & Piegari, L. (2022). Integrated electro-thermal model for li-ion battery packs. *Electronics*, *11*(10). doi: 10.3390/electronics11101537

Bernardi, D., Pawlikowski, E., & Newman, J. (1985, January). A General Energy Balance for Battery Systems. *Journal of The Electrochemical Society*, *132*(1), 5–12. doi: 10.1149/1.2113792

Damay, N., Forgez, C., Bichat, M.-P., Friedrich, G., & Ospina, A. (2013). Thermal modeling and experimental validation of a large prismatic li-ion battery. In *Iecon 2013 - 39th annual conference of the ieee industrial electronics society* (p. 4694-4699). doi: 10.1109/IECON.2013.6699893

Diederichsen, K. M., Buss, H. G., & McCloskey, B. D. (2017, May). The Compensation Effect in the Vogel–Tammann–Fulcher (VTF) Equation for Polymer-Based Electrolytes. *Macromolecules*, *50*(10), 3831–3840. doi: 10.1021/acs.macromol.7b00423

Forgez, C., Vinh Do, D., Friedrich, G., Morcrette, M., & Delacourt, C. (2010, May). Thermal modeling of a cylindrical LiFePO4/graphite lithium-ion battery. *Journal of Power Sources*, *195*(9), 2961–2968. doi: 10.1016/j.jpowsour.2009.10.105

García-Coln, L. S., del Castillo, L. F., & Goldstein, P. (1989, October). Theoretical basis for the Vogel-Fulcher-Tammann equation. *Physical Review B*, *40*(10), 7040–7044. doi: 10.1103/physrevb.40.7040

He, F., Li, X., & Ma, L. (2014, May). Combined experimental and numerical study of thermal management of battery module consisting of multiple Li-ion cells. *International Journal of Heat and Mass Transfer*, *72*, 622–629. doi: 10.1016/j.ijheatmasstransfer.2014.01.038

Hoelle, S., Dengler, F., Zimmermann, S., & Hinrichsen, O. (2023, jan). 3d thermal simulation of lithium-ion battery thermal runaway in autoclave calorimetry: Development and comparison of modeling approaches. *Journal of The Electrochemical Society*, *170*(1), 010509. doi: 10.1149/1945-7111/acac06

Hou, J., Yang, M., Wang, D., & Zhang, J. (2020). Fundamentals and challenges of lithium ion batteries at temperatures between -40° and 60°c. *Advanced Energy Materials*, *10*(18), 1904152. doi: https://doi.org/10.1002/aenm.201904152

Lam, L., Bauer, P., & Kelder, E. (2011, October). A practical circuit-based model for Li-ion battery cells in electric vehicle applications. In *2011 ieee 33rd international telecommunications energy conference (intelec).* IEEE. doi: 10.1109/intlec.2011.6099803

Li, D., Wang, L., Duan, C., Li, Q., & Wang, K. (2022). Temperature prediction of lithium-ion batteries based on electrochemical impedance spectrum: A review. *International Journal of Energy Research*, *46*(8), 10372-10388. doi: https://doi.org/10.1002/er.7905

Maleki, H., & Howard, J. N. (2006, October). Effects of overdischarge on performance and thermal stability of a Li-ion cell. *Journal of Power Sources*, *160*(2), 1395–1402. doi: 10.1016/j.jpowsour.2006.03.043

Paccha-Herrera, E., Calderón-Muñoz, W. R., Orchard, M., Jaramillo, F., & Medjaher, K. (2020, August). Thermal Modeling Approaches for a LiCoO2 Lithium-ion Battery—A Comparative Study with Experimental Validation. *Batteries*, *6*(3), 40. doi: 10.3390/batteries6030040

Pola, D., Guajardo, F., Jofré, E., Quintero, V., Pérez, A., Acuña, D., & Orchard, M. (2016). Particle-filtering-based state-of-health estimation and end-of-life prognosis for lithium-ion batteries at operation temperature. In *Annual Conference of the Prognostics and Health Management Society 2016* (p. 10).

Pola, D. A., Navarrete, H. F., Orchard, M. E., Rabié, R. S., Cerda, M. A., Olivares, B. E., ... Pérez, A. (2015). Particle-Filtering-Based Discharge Time Prognosis for Lithium-Ion Batteries With a Statistical Characterization of Use Profiles. *IEEE Transactions on Reliability*, *64*(2), 710–720. doi: http://dx.doi.org/10.1109/TR.2014.2385069

Qian, X., Xuan, D., Zhao, X., & Shi, Z. (2019, November). Heat dissipation optimization of lithium-ion battery pack based on neural networks. *Applied Thermal Engineering*, *162*, 114289. doi: 10.1016/j.applthermaleng.2019.114289

Spitthoff, L., Shearing, P. R., & Burheim, O. S. (2021). Temperature, ageing and thermal management of lithium-ion batteries. *Energies*, *14*(5). doi: 10.3390/en14051248

Spitthoff, L., Wahl, M. S., Lamb, J. J., Shearing, P. R., Vie, P. J. S., & Burheim, O. S. (2023, April). On the Relations between Lithium-Ion Battery Reaction Entropy, Surface Temperatures and Degradation. *Batteries*, *9*(5),

249. doi: 10.3390/batteries9050249

Wang, Y., Chen, X., Li, C., Yu, Y., Zhou, G., Wang, C., & Zhao, W. (2023). Temperature prediction of lithium-ion battery based on artificial neural network model. *Applied Thermal Engineering*, *228*, 120482. doi: 10.1016/j.applthermaleng.2023.120482

Yang, Z., Patil, D., & Fahimi, B. (2019). Electrothermal modeling of lithium-ion batteries for electric vehicles. *IEEE Transactions on Vehicular Technology*, *68*(1), 170-179. doi: 10.1109/TVT.2018.2880138

Zhang, Y., Song, W., & Feng, Z. (2013). An Energy Efficiency Evaluation Research Based on Heat Generation Behavior of Lithium-Ion Battery. *Journal of The Electrochemical Society*, *160*(11), A1927–A1930. doi: 10.1149/2.021311jes

Zhu, G., Kong, C., Wang, J. V., Kang, J., Yang, G., & Wang, Q. (2023). A fractional-order model of lithium-ion battery considering polarization in electrolyte and thermal effect. *Electrochimica Acta*, *438*, 141461. doi: https://doi.org/10.1016/j.electacta.2022.141461